

14 Three-Dimensional Radiative Transfer in Vegetation Canopies

Yuri Knyazikhin, Alexander Marshak, and Ranga B. Myneni

14.1 Introduction

Interaction of photons with a host medium is described by a linear transport equation. This equation has a very simple physical interpretation; it is a mathematical statement of the energy conservation law. In spite of the different physics behind radiation transfer in clouds and vegetation, these media have certain macro and micro-scale features in common. First, both are characterized by strong horizontal and vertical variations, and thus their three-dimensionality is important to correctly describe the photon transport. Second, the radiation regime is substantially influenced by the sizes of scattering centers that constitute the medium. Drop and leaf size distribution functions are the most important variables characterizing the micro-scale structure of clouds and vegetation canopies, respectively. Third, the independent (or incoherent) scattering concept underlies the derivation of the extinction coefficient and scattering phase function in both theories (van de Hulst, 1980, p. 4-5); (Ross, 1981, p. 144). This allows the transport equation to relate micro-scale properties of the medium to the photon distribution in the entire medium. From a mathematical point of view, these three features determine common properties of radiative transfer in clouds and vegetation.

However, the governing radiative transfer equation for leaf canopies, in both three-dimensional (3D) and one-dimensional (1D) geometries, has certain unique features. The extinction coefficient is a function of the direction of photon travel. Also, the differential scattering cross-section is not, as a rule, rotationally invariant, i.e., it generally depends on the absolute directions of photon travel Ω and Ω' , and not just the scattering angle $\arccos \Omega \bullet \Omega'$. Finally, the single scattering albedo is also a function of spatial and directional variables. These properties make solving of the radiative transfer equation more complicated; for example, the expansion of the differential scattering cross-section in spherical harmonics (see, Chap. 4) cannot be used.

In contrast to radiative transfer in clouds, the extinction coefficient in vegetation canopies introduced by Ross (1981) is wavelength independent, considering the size of scattering elements (leaves, branches, twigs, etc.) relative to the wavelength of solar radiation. Although the scattering and absorption processes are different at different wavelengths, the optical distance between two arbitrary points within the vegetation canopy does not depend on the wavelength. This spectral invariance

results in various unique relationships which, to some degree, compensate for difficulties in solving the radiative transfer equation due to the above mentioned features of the extinction and the differential scattering cross-sections.

We idealize a vegetation canopy as a medium filled with small planar elements of negligible thickness. We ignore all organs other than green leaves in this chapter. In addition, we neglect finite size of vegetation canopy elements. Thus, the vegetation canopy is treated as a gas with nondimensional planar scattering centers, i.e., a turbid medium. In other words, one cuts leaves resided in an elementary volume into “dimensionless pieces” and uniformly distributes them within the elementary volume. Two variables, the leaf area density distribution function and the leaf normal distribution are used in the theory of radiative transfer in vegetation canopies to convey “information” about the total leaf area and leaf orientations in the elementary volume before “converting the leaves into the gas.”

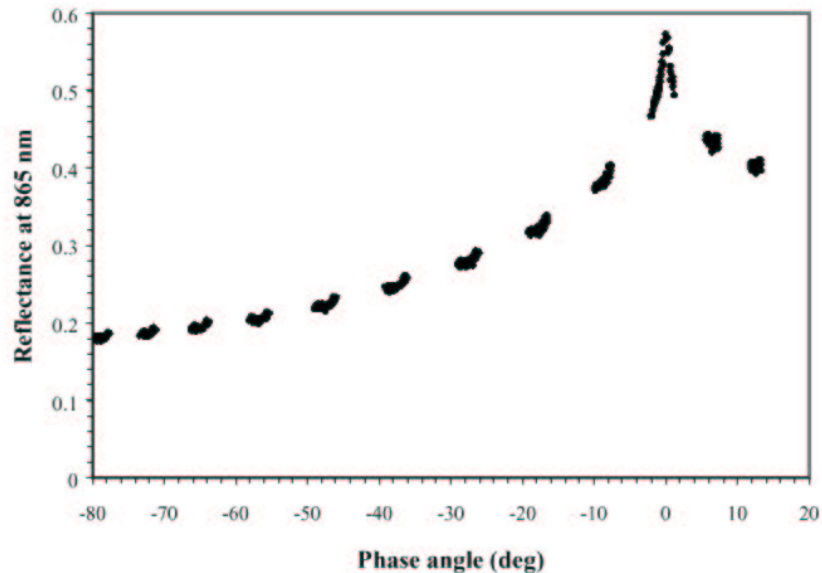


Fig. 14.1. Mean reflectance of evergreen broadleaf forest at near-infrared (865nm) wavelength as a function of phase angle (after Bréon et al., 2001)). Data were acquired by the POLDER (Polarization and Directionality of the Earth’s Reflectances) multi-angle spaceborne instrument (Deschamps et al., 1994). Phase angles are shown with a negative sign if the POLDER view azimuth was greater than 180°. Canopy reflectances exhibit a sharp peak about the retro-illumination direction (the “hot spot ”effect) which classical transport equation can not predict.

It should be noted that the turbid medium assumption is violated in the case of vegetation canopies and, therefore, finite size scatters can cast shadows. This causes a very sharp peak in reflected radiation about the retro-solar direction. This phenomenon is referred to as the “hot spot” effect (Fig. 14.1). It is clear that point scatters cannot cast shadows and thus, the turbid medium concept in its original formulation (Ross, 1981) fails to predict or duplicate experimental observation of exiting radiation about the retro-illumination direction (Kuusk, 1985; Gerstl and Simmer, 1986; Marshak, 1989; Verstrate et al., 1990). Recently, Zhang et al. (2002) showed that if the solution to the radiative transfer equation is treated as a Schwartz distribution, then an additional term must be added to the solution of the radiative transfer equation. This term describes the hot spot effect. This result justifies the use of the transport equation as the basis to model canopy-radiation regime. Here we will follow classical radiative transfer theory in vegetation canopies proposed by Ross (1981) with emphasis on canopy spectral response to the incident radiation. For the mathematical theory of Schwartz distributions applicable to the transport equation, the reader is referred to Germogenova (1986), Choulli and Stefanov (1996) and Antyufeev and Bondarenko (1996).

Finally, what are our motivations to include a chapter on radiative transfer in vegetation canopies in the book on atmospheric radiative transfer? Why is the vegetation canopy a special type of surface? First of all, vegetated surfaces play an important role in the Earth’s energy balance and have a significant impact on the global carbon cycle. The problem of accurately evaluating the exchange of carbon between the atmosphere and terrestrial vegetation has received scientific (Intergovernmental Panel on Climate Change (IPCC), 1995) and, also, political attention (Steffen et al., 1998). The next motivation is both the similarity and the unique features of the radiative transfer equations that govern radiative transfer processes in these neighbouring media. Because of their radiative interactions, the vegetation canopy and the atmosphere are coupled together; each serves as a boundary condition to the radiative transfer equations in the adjacent medium. To better understand radiative processes in these media we need an accurate description of their interactions. This chapter complements the rest of the book and mainly deals with radiative transfer in vegetation canopies. The last section outlines a technique needed to describe the canopy-clouds interaction.

14.2 Vegetation Canopy Structure and Optics

Solar radiation scattered from a vegetation canopy results from interaction of photons traversing through the foliage medium, bounded at the bottom by a radiatively participating surface. Therefore to estimate the canopy radiation regime, three important features must be carefully formulated. They are (1) the architecture of individual plants and of the entire canopy; (2) optical properties of vegetation elements (leaves, stems) and soil; the former depends on physiological conditions (water status, pigment concentration); and (3) atmospheric conditions which determine the incident radiation field (Ross, 1981). For radiative transfer in clouds, they correspond

respectively to cloud micro (e.g., distribution of cloud drop sizes) and macro (e.g., cloud type and geometry) structures, cloud drop optical properties, and boundary (illumination) conditions. Note that radiation incident on the top of the atmosphere is a monodirectional solar beam while the vegetation canopies are illuminated both by monodirectional beam attenuated by the atmosphere and radiation scattered by the atmosphere (diffuse radiation). Photon transport theory aims at deriving the solar radiation regime, both within the vegetation canopy and cloudy atmosphere, using the above mentioned attributes as input data. For vegetation canopy, the leaf area density distribution, u_L , leaf normal orientation distribution, g_L , leaf scattering phase function, γ_L , and boundary conditions specify these input (Ross, 1981; Myneni et al., 1990; Knyazikhin, 1991; Pinty and Verstraete, 1997). We will start with definitions of these variables.

14.2.1 Vegetation Canopy Structure

At the very least, two important wavelength independent structural attributes - leaf area density and leaf normal orientation distribution functions - need to be defined in order to quantify vegetation-photon interactions.

The one-sided green leaf area per unit volume in the vegetation canopy at location $\mathbf{x} = (x, y, z)$ is defined as the leaf area density distribution $u_L(\mathbf{x})$ (in m^2/m^3 or simply m^{-1}). Realistic modeling of $u_L(\mathbf{x})$ is a challenge for it requires simulated vegetation canopies with computer graphics and tedious field measurements. The dimensionless quantity

$$L(x, y) = \int_0^H dz u_L(x, y, z), \quad (14.1)$$

is called the *leaf area index*, one-sided green leaf area per unit ground area at (x, y) . Here H is depth of the vegetation canopy.

Figures 14.2 and 14.3 demonstrate a computer-generated Norway spruce stand and corresponding leaf area index $L(x, y)$ at a spatial resolution of 50 cm (i.e., distribution of the mean leaf area index $L(x, y)$ taken over each of 50 by 50 cm ground cells). Leaf area index is the key variable in most ecosystem productivity models, and in global models of climate, hydrology, biogeochemistry and ecology which attempt to describe the exchange of fluxes of energy, mass (e.g., water and CO_2), and momentum between the surface and the atmosphere. In order to quantitatively and accurately model global dynamics of these processes, differentiate short-term from long-term trends as well as to distinguish regional from global phenomena, this parameter must be collected often for a long period of time and should represent every region of the Earth land surface. The leaf area index has been operationally produced from data provided by two instruments, the moderate resolution imaging spectroradiometer (MODIS) and multiangle imaging spectroradiometer (MISR), during the Earth Observing System (EOS) Terra mission (Myneni et al., 2002). Global map of MODIS leaf area index at 1 km resolution is shown in Fig. 14.4. Note that the theory of radiative transfer in vegetation canopies presented in this chapter underlies

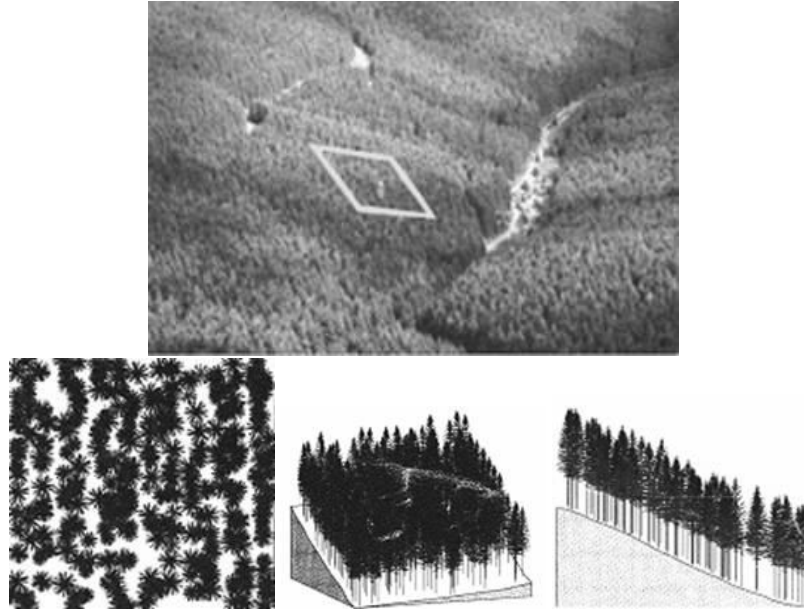


Fig. 14.2. Photo shows a Norway spruce stand about 50 km of Goettingen in the Harz mountains. The forest is about 45 years old and situated on the south slope. For the sake of detailed examination of the canopy structure, a site covering an area of approximately $40 \times 40 \text{ m}^2$ was chosen (shown as a square) and taken as representative for the whole stand. The canopy space is limited by the slope and a plane parallel to the slope at the height of the tallest tree of 12.5 m. There are in total 297 trees in the sample stand. The tree trunk diameters varied from 6 to 28 cm. The stand is rather dense but with some localized gaps. For the needs of modeling the trees were divided into five groups with respect to the tree trunk diameter. A model of a Norway spruce based on fractal theory was then used to build a representative of each group (Kranigk and Gravenhorst, 1993; Kranigk et al., 1994; Knyazikhin et al., 1996). Given the distribution of tree trunks in the stand, the diameter of each tree, the entire sample site was generated. Bottom panels demonstrate the computer generated Norway spruce stand shown from different directions: crown map (left panel), front view (middle panel), and cross section (right panel).

the retrieval technique for retrieving leaf area index from satellite data (Knyazikhin, 1991; Knyazikhin and Marshak, 1991).

Let Ω_L be the upward normal to the leaf element. The following function characterizes the leaf normals distribution: $(1/2\pi)g_L(\Omega_L)$ is the probability density of the leaf normals distribution with respect to the upward hemisphere (Ξ_+)

$$\frac{1}{2\pi} \int_{\Xi_+} d\Omega_L g_L(\Omega_L) = 1. \quad (14.2)$$

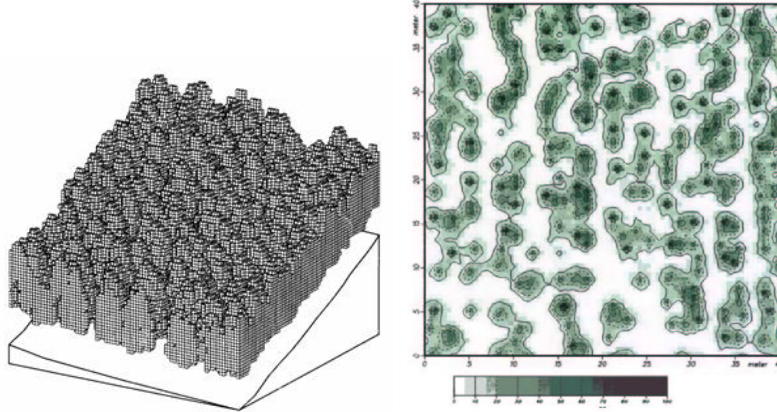


Fig. 14.3. A fine spatial mesh of the resolution of $50 \times 50 \times 50$ cm was imposed on the computer generated sample site shown in Fig. 14.2 and the leaf area density $u_L(\mathbf{x})$ in each of the fine cells was evaluated. The canopy space contains 160,000 fine cells. The left panel shows three-dimensional distribution of foliated cells. This distribution is described by an indicator function $\chi(\mathbf{x})$ whose value is 1 if $u_L(\mathbf{x}) \neq 0$, and 0 otherwise. The leaf area index $L(x, y)$ (14.1) derived from the computer generated leaf area density $u_L(\mathbf{x})$ is shown in the right panel.

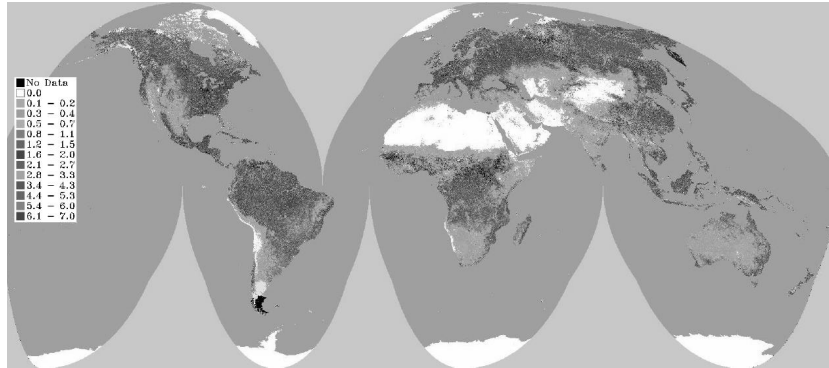


Fig. 14.4. Color-coded map of the leaf area index at 1 km resolution for July 20-27, 2001, derived from data acquired by the moderate resolution imaging spectroradiometer (MODIS) on board the Earth Observing System (EOS) Terra platform.

If the polar angle θ_L and azimuth ϕ_L of the normal Ω_L are assumed independent, then

$$\frac{1}{2\pi} g_L(\Omega_L) = \bar{g}_L(\theta_L) \frac{1}{2\pi} h_L(\phi_L), \quad (14.3)$$

where $\bar{g}_L(\theta_L)$ and $(1/2\pi)h_L(\phi_L)$ are the *probability density functions of leaf normal inclination* and *azimuth*, respectively, and

$$\int_0^{\pi/2} \bar{g}_L(\theta_L) \sin \theta_L d\theta_L = 1, \quad \frac{1}{2\pi} \int_0^{2\pi} h_L(\phi_L) d\phi_L = 1. \quad (14.4)$$

The functions $g_L(\Omega_L)$, $\bar{g}_L(\theta_L)$ and $h_L(\phi_L)$ depend on the location x in the vegetation canopy but this is implicit in the remainder of the text.

The following example model distribution functions for leaf normal inclination were proposed by DeWit (1965): *planophile* - mostly horizontal leaves, *erectophile* - mostly erect leaves; *plagiophile* - mostly leaves at 45 degrees; *extremophile* - mostly horizontal and vertical leaves; and *uniform* - all possible inclinations. These distributions can be expressed as (cf. Bunnik, 1978),

$$\text{Planophile: } \bar{g}_L(\theta_L) = \frac{2}{\pi} (1 + \cos 2\theta_L), \quad (14.5a)$$

$$\text{Erectophile: } \bar{g}_L(\theta_L) = \frac{2}{\pi} (1 - \cos 2\theta_L), \quad (14.5b)$$

$$\text{Plagiophile: } \bar{g}_L(\theta_L) = \frac{2}{\pi} (1 - \cos 4\theta_L), \quad (14.5c)$$

$$\text{Extremophile: } \bar{g}_L(\theta_L) = \frac{2}{\pi} (1 + \cos 4\theta_L), \quad (14.5d)$$

$$\text{Uniform: } \bar{g}_L(\theta_L) = 1. \quad (14.5e)$$

Example distributions of the leaf normal inclination are shown in Fig. 14.5.

Certain plants, such as soybeans and sunflowers, exhibit heliotropism, where the leaf azimuths have a preferred orientation with respect to the solar azimuth. A simple model for h_L in such canopies is $h_L(\phi_L, \phi_0) = 2 \cos^2(\phi_0 - \phi_L - \eta)$ where the parameter η is the difference between the azimuth of the maximum of the distribution function h_L and the fixed azimuth of the incident photon ϕ_0 (cf. Verstraete, 1987). In the case of diaheliotropic distributions, which tend to maximize the projected leaf area to the incident stream $\eta = 0$. On the other hand, paraheliotropic distributions tends to minimize the leaf area projected to the incident stream, $\eta = \pi/2$. A more general model for the leaf normal orientations is the β -distribution, the parameters of which can be obtained from fits to field measurements of the leaf normal orientation (Goel and Strelbel, 1984).

14.2.2 Vegetation Canopy Optics

A photon incident on a leaf surface can either be absorbed or scattered. If the scattered photon emerges from the same side of the leaf as the incident photon, the event is termed reflection. Likewise, if the scattered photon exits the leaf from the opposite side, the event is termed transmission. Scattering of solar radiation by green leaves does not involve frequency shifting interactions, but is dependent on the wavelength.

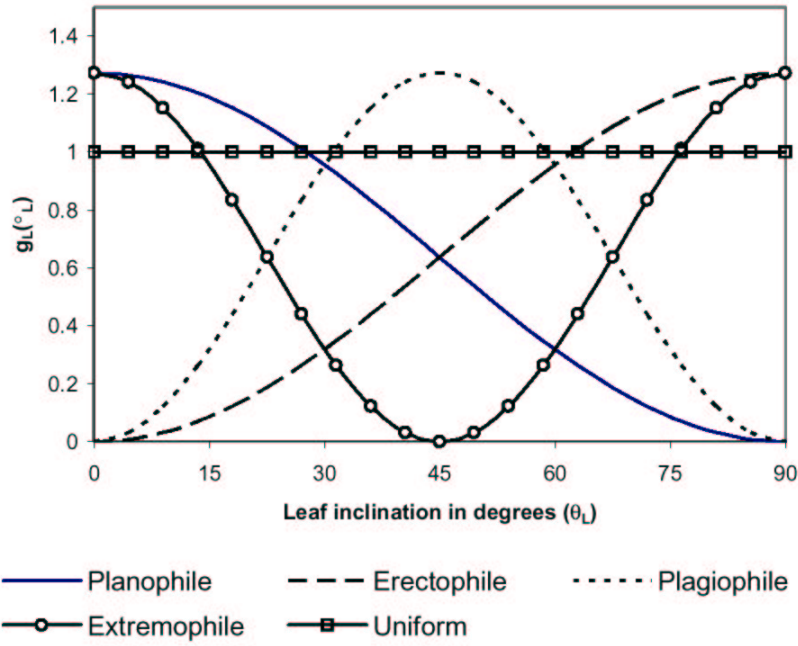


Fig. 14.5. The probability density functions for planophile (14.5a), erectophile (14.5b), plagiophile (14.5c), extremophile (14.5d) and uniform (14.5e) distributions.

The angular distribution of radiant energy scattered by a leaf element is a key variable, and is specified by the leaf element scattering phase function $\gamma_{L,\lambda}(\Omega' \rightarrow \Omega, \Omega_L)$. For a leaf with upward normal Ω_L , this phase function is the fraction of intercepted energy, from photon initially traveling in Ω' , that is scattered into an element of solid angle $d\Omega$ about Ω .

Radiant energy may be incident on the upper or the lower sides of the leaf element and the scattering event may be either reflection or transmission. Integration of the leaf scattering phase function over the appropriate solid angles gives the *hemispherical leaf reflectance* $\rho_{L,\lambda}(\Omega', \Omega_L)$ and *transmittance* $\tau_{L,\lambda}(\Omega', \Omega_L)$ coefficients. The leaf scattering phase function when integrated over all scattered photon directions (Ξ) yields the leaf albedo,

$$\omega_{L,\lambda}(\Omega', \Omega_L) = \int_{\Xi} \gamma_{L,\lambda}(\Omega' \rightarrow \Omega, \Omega_L) d\Omega \quad (14.6)$$

where Ξ is the unit sphere. The leaf albedo $\omega_{L,\lambda}(\Omega', \Omega_L)$ is simply the sum of $\rho_{L,\lambda}(\Omega', \Omega_L)$ and $\tau_{L,\lambda}(\Omega', \Omega_L)$. The reflectance and transmittance of an individual leaf depends on wavelength, tree species, growth conditions, leaf age and its location in the canopy.

A photon incident on a leaf element can either be specularly reflected from the surface depending on its roughness or emerge diffused from interactions in the leaf interior. Some leaves can be quite smooth from a coat of wax-like material, while other leaves can have hairs making the surface rough. Light reflected from the leaf surface can be polarized as well. Photons that do not suffer leaf surface reflection enter the interior of the leaf, where they are either absorbed or refracted because of the many refractive index discontinuities between the cell walls and intervening air cavities. Photons that are not absorbed in the interior of the leaf emerge on both sides, generally diffused in all directions. Figure 14.6 shows typical diffuse hemispherical reflectance, $\rho_{L,\lambda}(-\Omega_L, \Omega_L)$, and transmittance, $\tau_{L,\lambda}(-\Omega_L, \Omega_L)$, spectra of an individual leaf under normal illumination. For more details on diffuse leaf scattering and specular reflection from the leaf surface, the reader is referred to Walter-Shea and Norman (1991), and Vanderbilt et al. (1991).

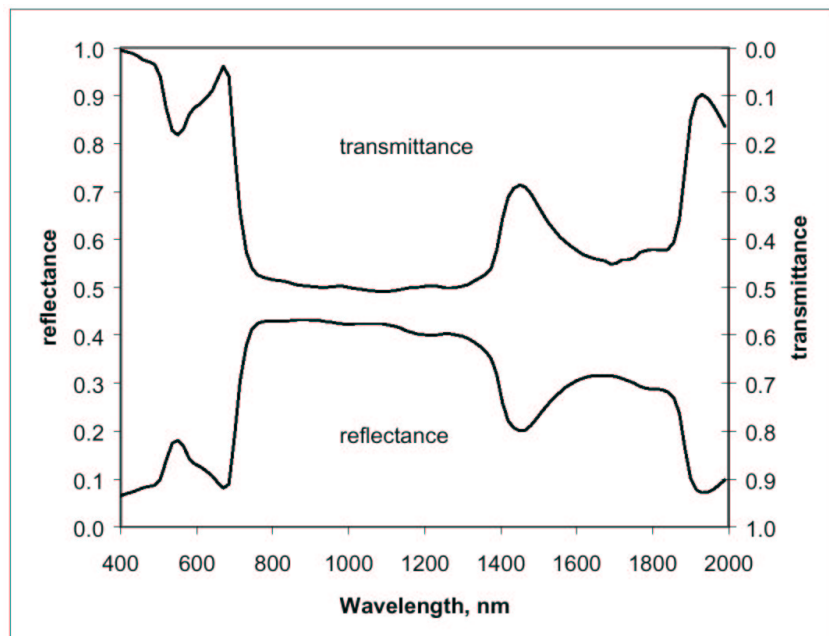


Fig. 14.6. Typical reflectance and transmittance spectra of an individual plant leaf from 400 to 2000 nm for normal incidence.

14.2.3 Extinction, Scattering and Absorption Events

To derive an expression for the extinction coefficient consider photons at x traveling along Ω . The total extinction coefficient is the probability, per unit path length of

travel, that the photon encounters a leaf element,

$$\sigma(\mathbf{x}, \Omega) = u_L(\mathbf{x}) G(\mathbf{x}, \Omega), \quad (14.7)$$

where $G(\mathbf{x}, \Omega)$ is the *geometry factor* first proposed by Ross (1981), defined as the projection of unit leaf area at \mathbf{x} onto a plane perpendicular to the direction of photon travel Ω , i.e.,

$$G(\mathbf{x}, \Omega) = \frac{1}{2\pi} \int_{\Xi_+} d\Omega_L g_L(\mathbf{x}, \Omega_L) |\Omega \bullet \Omega_L|. \quad (14.8)$$

The geometry factor G satisfies $(2\pi)^{-1} \int_{\Xi_+} G(\mathbf{x}, \Omega) d\Omega = 1/2$. Upon collision with a leaf element, a photon can be either absorbed or scattered. So the extinction coefficient can be broken down into its scattering and absorption components, $\sigma = \sigma_{s,\lambda} + \sigma_{a,\lambda}$. It is important to note that the geometry factor is an explicit function of the direction of photon travel Ω in the general case of non-uniformly distributed leaf normals. This imbues directional dependence to the extinction coefficients in the case of vegetation canopies. Only in the case of uniformly distributed leaf normals ($G = 1/2$) its dependence on Ω disappears. A noteworthy point is the *wavelength independence* of σ , that is, the extinction probabilities for photons in vegetation media are determined by the structure of the canopy rather than photon frequency or the optics of the canopy.

Consider photons impinging on leaf elements of area density u_L at location \mathbf{x} along Ω' . The probability density, per unit path length, that these photons would be intercepted and then scattered in to the direction Ω is given by the differential scattering coefficient

$$\begin{aligned} \sigma'_{s,\lambda}(\mathbf{x}, \Omega' \rightarrow \Omega) &= u_L(\mathbf{x}) \frac{1}{\pi} \Gamma_\lambda(\mathbf{x}, \Omega' \rightarrow \Omega), \\ &= u_L(\mathbf{x}) \frac{1}{2\pi} \int_{\Xi_+} d\Omega_L g_L(\mathbf{x}, \Omega_L) |\Omega' \bullet \Omega_L| \gamma_{L,\lambda}(\Omega' \rightarrow \Omega, \Omega_L), \end{aligned} \quad (14.9)$$

where $(1/\pi)\Gamma_\lambda$ is the *area scattering phase function* first proposed by Ross (1981). The scattering phase function combines diffuse scattering from the interior of a leaf and specular reflection from the leaf surface. For more details on the diffuse and specular components of the area scattering phase function, the reader is referred to Ross (1981), Marshak (1989), Myneni (1991), Knyazikhin and Marshak (1991).

It is important to note that the differential scattering coefficient is an explicit function of the polar coordinates of Ω' and Ω , that is, non-rotationally invariant. Only in some limited cases it can be reduced to the rotationally invariant form, $\sigma'_{s,\lambda}(\mathbf{x}, \Omega \rightarrow \Omega') \equiv \sigma'_{s,\lambda}(\mathbf{x}, \Omega \bullet \Omega')$. This property precludes the use of Legendre polynomial expansions and of the addition theorem often used in transport theory for handling the scattering integral (see, Chap. 4).

Integration of the differential scattering coefficient (14.9) over all scattered photon directions results in the scattering coefficient,

$$\sigma_{s,\lambda}(\mathbf{x}, \Omega) = u_L(\mathbf{x}) \frac{1}{2\pi} \int_{\Xi_+} d\Omega_L g_L(\mathbf{x}, \Omega_L) |\Omega \bullet \Omega_L| \omega_{L,\lambda}(\Omega, \Omega_L). \quad (14.10)$$

The absorption coefficient can be specified as

$$\begin{aligned} \sigma_{a,\lambda}(\mathbf{x}, \Omega) &= \sigma(\mathbf{x}, \Omega) - \sigma_{s,\lambda}(\mathbf{x}, \Omega) \\ &= u_L(\mathbf{x}) \frac{1}{2\pi} \int_{\Xi_+} d\Omega_L g_L(\mathbf{x}, \Omega_L) |\Omega \bullet \Omega_L| [1 - \omega_{L,\lambda}(\Omega, \Omega_L)]. \end{aligned} \quad (14.11)$$

The magnitude of scattering by leaves in an elementary volume is described by using the single scattering albedo defined as the ratio of energy scattered by an elementary volume to energy intercepted by this volume

$$\begin{aligned} \varpi_{0,\lambda}(\mathbf{x}, \Omega) &= \frac{\sigma_{s,\lambda}(\mathbf{x}, \Omega)}{\sigma_{s,\lambda}(\mathbf{x}, \Omega) + \sigma_{a,\lambda}(\mathbf{x}, \Omega)} \\ &= \frac{\int_{\Xi_+} d\Omega_L g(\mathbf{x}, \Omega_L) |\Omega \bullet \Omega_L| \omega_{L,\lambda}(\Omega, \Omega_L)}{\int_{\Xi_+} d\Omega_L g(\mathbf{x}, \Omega_L) |\Omega \bullet \Omega_L|}. \end{aligned}$$

Given the single scattering albedo, the scattering and absorption coefficients can be expressed via the extinction coefficient as

$$\sigma_{s,\lambda}(\mathbf{x}, \Omega) = \varpi_{0,\lambda}(\mathbf{x}, \Omega) \sigma(\mathbf{x}, \Omega), \quad (14.12a)$$

$$\sigma_{a,\lambda}(\mathbf{x}, \Omega) = [1 - \varpi_{0,\lambda}(\mathbf{x}, \Omega)] \sigma(\mathbf{x}, \Omega). \quad (14.12b)$$

Note that only if the leaf albedo $\omega_{L,\lambda}$ defined by (14.6) does not depend on the leaf normal Ω_L , will the single scattering albedo coincides with the leaf albedo, i.e. $\varpi_{0,\lambda}(\mathbf{x}, \Omega) \equiv \omega_{L,\lambda}(\mathbf{x}, \Omega)$.

14.3 Radiative Transfer in Vegetation Canopies

Let the domain V in which a vegetation canopy is located, be a parallelepiped of horizontal dimensions X_S , Y_S , and height Z_S . The top ∂V_t , bottom ∂V_b , and lateral ∂V_l surfaces of the parallelepiped form the canopy boundary $\partial V = \partial V_t + \partial V_b + \partial V_l$. Note the boundary ∂V is excluded from the definition of V . The function characterizing the radiative field in V is the monochromatic intensity $I_\lambda(\mathbf{x}, \Omega)$ depending on wavelength, λ , location \mathbf{x} and direction Ω . Assuming no polarization and emission within the canopy, the monochromatic intensity distribution function is given by the

steady-state radiative transfer equation (Ross, 1981; Myneni et al., 1990; Myneni, 1991):

$$\Omega \bullet \nabla I_\lambda(\mathbf{x}, \Omega) + G(\mathbf{x}, \Omega) u_L(\mathbf{x}) I_\lambda(\mathbf{x}, \Omega) = \frac{u_L(\mathbf{x})}{\pi} \int_{\Xi} \Gamma_\lambda(\mathbf{x}, \Omega' \rightarrow \Omega) I_\lambda(\mathbf{x}, \Omega') d\Omega'. \quad (14.13)$$

14.3.1 Boundary Value Problem for Radiative Transfer Equation in the Vegetation Canopy

Equation (14.3) alone does not provide a full description of the radiative transfer process. It is necessary to specify the incident radiation at the canopy boundary, ∂V , i.e. specification of the boundary conditions. Because the canopy is adjacent to the atmosphere, a neighboring canopy, and the soil, all of which have different reflection properties, the following boundary conditions are used to describe the incoming radiation ((Kranigk et al., 1994; Knyazikhin et al., 1997)):

$$I_\lambda(\mathbf{x}_t, \Omega) = I_{0,d,\lambda}(\mathbf{x}_t, \Omega) + I_{0,\lambda}(\mathbf{x}_t) \delta(\Omega - \Omega_0), \mathbf{x}_t \in \partial V_t, \Omega \bullet \mathbf{n}_t < 0, \quad (14.14a)$$

$$I_\lambda(\mathbf{x}_l, \Omega) = \frac{1}{\pi} \int_{\Omega' \bullet \mathbf{n}_l > 0} \rho_{\lambda,l}(\Omega', \Omega) I_\lambda(\mathbf{x}_l, \Omega') |\Omega' \bullet \mathbf{n}_l| d\Omega' + L_{d,\lambda}(\mathbf{x}_l, \Omega) \\ + L_{m,\lambda}(\mathbf{x}_l) \delta(\Omega - \Omega_0), \mathbf{x}_l \in \partial V_l, \Omega \bullet \mathbf{n}_l < 0, \quad (14.14b)$$

$$I_\lambda(\mathbf{x}_b, \Omega) = \frac{1}{\pi} \int_{\Omega' \bullet \mathbf{n}_b > 0} \rho_{\lambda,b}(\Omega', \Omega) I_\lambda(\mathbf{x}_b, \Omega') |\Omega' \bullet \mathbf{n}_b| d\Omega', \mathbf{x}_b \in \partial V_b, \Omega \bullet \mathbf{n}_b < 0, \quad (14.14c)$$

where $I_{0,d,\lambda}$ and $I_{0,\lambda}$ are intensities of the diffuse and monodirectional components of solar radiation incident on the top of the canopy boundary, ∂V_t ; Ω_0 denotes direction of the monodirectional solar component; δ is the Dirac delta-function; $L_{m,\lambda}(\mathbf{x}_t)$ is the intensity of the monodirectional solar radiation arriving at a point $\mathbf{x}_l \in \partial V_l$ along Ω_0 without experiencing an interaction with the neighboring canopies; $L_{d,\lambda}$ is the diffuse radiation penetrating through the lateral surface in the stand; $\rho_{\lambda,l}$ and $\rho_{\lambda,b}$ (sr^{-1}) are the bi-directional reflectance factors of the lateral and the bottom surfaces; \mathbf{n}_t , \mathbf{n}_l and \mathbf{n}_b are the outward normals at points $\mathbf{x}_t \in \partial V_t$, $\mathbf{x}_l \in \partial V_l$, and $\mathbf{x}_b \in \partial V_b$, respectively.

A neighboring environment as well as the fraction of the monodirectional solar radiation in the total incident radiation influences the radiative regime in the vegetation canopy. In order to demonstrate a range of this influence we simulate two extreme situations for a 40 m by 40 m sample stand shown in Fig. 14.2. In the first one, we “cut” the forest surrounding the sample plot. The incoming solar radiation can reach the sides of the sample stand without experiencing a collision in this case. The boundary condition (14.13) with $\rho_{\lambda,l} = 0$, $L_{d,\lambda} = I_{0,d,\lambda}$, and $L_{m,\lambda} = I_{0,\lambda}$ was used to describe photons penetrating into the canopy through the lateral surface.

In the second situation, we “plant” a forest of an extremely high density around the sample stand so that no solar radiation can penetrate into the stand through the lateral boundary ∂V_l . The lateral boundary condition (14.13) takes the form $I(\mathbf{x}_l, \Omega) = 0$. The radiative regimes in a real stand usually vary between these extreme situations. For each situation, the boundary value problem (14.3)-(14.13) was solved and a vertical profile of mean downward radiation flux density was evaluated. Figure 14.7 demonstrates downward fluxes normalized by the incident flux at noon on a cloudy and on a clear sunny day. A downward radiation flux density evaluated by averaging the extinction coefficient (14.7) and area scattering phase function (14.9) over the 40 m by 40 m area first and then solving a one-dimensional radiative transfer equation is also plotted in this figure. One can see that the radiative regime in the sample stand is more sensitive to the lateral boundary conditions during cloudy days. In both cases, a 3D medium transmits more radiation than those predicted by the 1D transport equation. This is consistent with radiation transmitted through inhomogeneous clouds (see, Chap. 9) and with Jensen inequality (@@.@@).

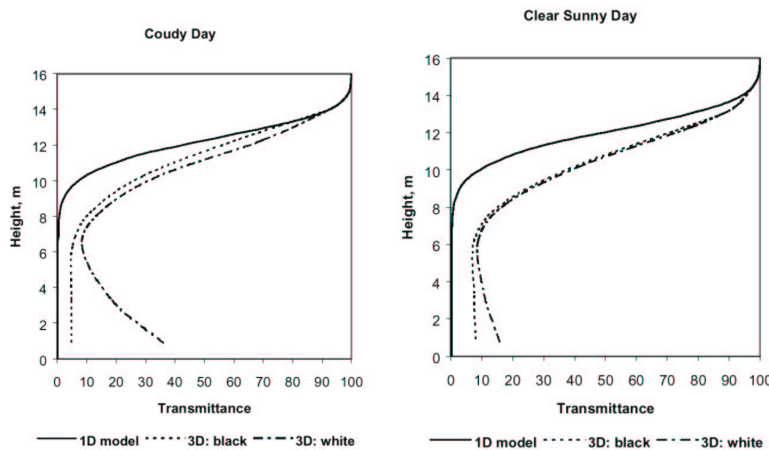


Fig. 14.7. Vertical profile of the downward radiation flux normalized by the incident flux derived from the one-dimensional (legend “1D model”) and three-dimensional (legends “3D black” and “3D white”) models on a cloudy day and on a clear sunny day. Curves “3D: black” correspond to a forest stand surrounded by the optically black lateral boundary, and curves “3D: white” to an isolated forest stand of the same size and structure.

The radiation penetrating through the lateral sides of the canopy depends on the neighboring environment. Its influence on the radiation field within the canopy is especially pronounced near the lateral canopy boundary. Therefore inaccuracies in the lateral boundary conditions may cause distortions in the simulated radiation field within the domain V . These features should be taken into account when 3D radiation distribution in a vegetation canopy of a small area is investigated. The problem of photon transport in such canopies arises, for example, in the context of

optimal planting and cutting of industrial wood (Knyazikhin et al., 1994), land surface climatology, and plant physiology. The lateral side effects, however, decrease with distance from this boundary toward the center of the domain. The size of the “distorted area” depends on the adjoining vegetation and atmospheric conditions (Kranigk, 1996). In particular, it has been shown that these lateral effects can be neglected when the radiation regime is analyzed in a rather extended canopy (see, Chap. 9 for comparison with clouds). A “zero” boundary condition for the lateral surface can then be used to simulate canopy radiation regime.

14.3.2 Reflection of Vegetated Surfaces

Solution of the boundary value problem (14.3)-(14.13), describes the radiative regime in a vegetation canopy and, as a consequence, reflectance properties of the vegetation canopy. As it was demonstrated in Fig. 14.7, the canopy-radiation regime is sensitive to the partition between the monodirectional and diffuse components of the incoming radiation. The ratio $f_{\text{dir},\lambda}$ of the monodirectional to the total radiation flux incident on the canopy is used to parameterize canopy reflectance properties; that is,

$$f_{\text{dir},\lambda} = \frac{\int_{\partial V_t} I_{0,\lambda}(\mathbf{x}_t) |\mu_0| d\mathbf{x}_t}{\int_{\partial V_t} I_{0,\lambda}(\mathbf{x}_t) |\mu_0| d\mathbf{x}_t + \int_{\partial V_t} d\mathbf{x}_t \int_{\mathbf{n}_t \bullet \Omega < 0} I_{0,d,\lambda}(\mathbf{x}_t, \Omega) |\mathbf{n}_t \bullet \Omega| d\Omega}. \quad (14.15)$$

The hemispherical-directional reflectance factor (HDRF, dimensionless) for non-isotropic incident radiation is defined as the ratio of the mean radiance leaving the top of the plant canopy to the mean radiance reflected from an ideal Lambertian target into the same beam geometry and illuminated under identical atmospheric conditions (Martonchik et al., 2000); this can be expressed by the solution of (14.10)-(14.11) as

$$r_\lambda(\Omega) = \frac{\int_{\partial V_t} I_\lambda(\mathbf{x}_t, \Omega) d\mathbf{x}_t}{\frac{1}{\pi} \int_{\partial V_t} d\mathbf{x}_t \int_{\mathbf{n}_t \bullet \Omega' < 0} I_\lambda(\mathbf{x}_t, \Omega') |\Omega' \bullet \mathbf{n}_t| d\Omega'}, \Omega \bullet \mathbf{n}_t > 0. \quad (14.16)$$

The bihemispherical reflectance for nonisotropic incident radiation (BHR, dimensionless) is defined as the ratio of the exiting flux to the incident flux (Martonchik et al., 2000); that is,

$$R(\lambda) = \frac{\int_{\partial V_t} d\mathbf{x}_t \int_{\mathbf{n}_t \bullet \Omega' > 0} I_\lambda(\mathbf{x}_t, \Omega') |\Omega' \bullet \mathbf{n}_t| d\Omega'}{\int_{\partial V_t} d\mathbf{x}_t \int_{\mathbf{n}_t \bullet \Omega' < 0} I_\lambda(\mathbf{x}_t, \Omega') |\Omega' \bullet \mathbf{n}_t| d\Omega'}. \quad (14.17)$$

The HDRF and BHR depend on the ratio f_{dir} of monodirectional irradiance on the top of the vegetation canopy to the total incident irradiance. If $f_{\text{dir}} = 1$, the HDRF and BHR become the bidirectional reflectance factor (BRF, dimensionless) and the directional hemispherical reflectance (DHR, dimensionless), respectively. These variables can be derived from data acquired by satellite-borne sensors (Diner et al., 1999) which, in turn, are input to various techniques for retrieval of biophysical parameters from space. It should be noted that the HDRF and BHR, in general,

depend on the direction Ω_0 of solar beam. However, HDRF=BRF=DHR=BHR for Lambertian surfaces.

In remote sensing, the dimension of the upper boundary ∂V_t coincides with a footprint of the imagery. Tending ∂V_t to zero results in a BRF value defined at a given spatial point x_t . Such a BRF is used to describe the lower boundary condition for the radiative transfer in the atmosphere (Sect. 14.5).

14.4 Canopy Spectral Invariants

The extinction coefficient in vegetation canopies is treated as wavelength independent considering the size of the scattering elements (leaves, branches, twigs, etc.) relative to the wavelength of solar radiation. This results in canopy spectral invariants stating that some simple algebraic combinations of the single scattering albedo and canopy spectral transmittances and reflectances eliminate their dependencies on wavelength through the specification of canopy-specific wavelength independent variables. These variables specify an accurate relationship between the spectral response of a vegetation canopy to incident solar radiation at the leaf and the canopy scale. In terms of these variables, the partitioning of the incident solar radiation into canopy transmission and interception can be described by expressions which relate canopy transmittance and interception at an arbitrary wavelength to transmittances and interceptions at all other wavelengths in the solar spectrum (Knyazikhin et al., 1998b; Panferov et al., 2001; Shabanov et al., 2003). Furthermore; the canopy spectral invariants allows to separate a small set of independent variables that fully describes the law of energy conservation in vegetation canopies at any wavelength in the visible and near-infrared part of the solar spectrum (Wang et al., 2003). These characteristic features of radiative transfer in vegetation canopies are discussed in this section.

14.4.1 Canopy Spectral Behavior in the Case of an Absorbing Ground

Consider a vegetation canopy confined to $0 < z < H$. The plane surface $z = 0$ and $z = H$ constitute its upper and lower boundaries, respectively. In other words, a “horizontally extended” area is considered; thus no lateral illumination is assumed or needed. The spectral composition of the incident radiation is altered by interactions with phytoelements. The magnitude of scattering by the foliage elements is characterized by the hemispherical leaf reflectance and transmittance introduced earlier. The reflectance and transmittance of an individual leaf depends on wavelength, tree species, growth conditions, leaf age and its location in the canopy. We start with the simplest case where reflectance of the ground below the vegetation is zero. Results presented in this subsection are required to extend our analysis to the general case of a reflecting ground below the vegetation.

Let a parallel beam of unit intensity be incident on the upper boundary in the direction Ω_0 . Equation (14.3) describes the radiative transfer process within the

vegetation canopy. In this case, the boundary conditions are simpler than in (14.13) - (14.13):

$$I_\lambda(\mathbf{x}_t, \Omega) = \delta(\Omega - \Omega_0), \quad \mathbf{x}_t \in \partial V_t, \Omega \bullet \mathbf{n}_t < 0, \quad (14.18a)$$

$$I_\lambda(\mathbf{x}_b, \Omega) = 0, \quad \mathbf{x}_b \in \partial V_b, \Omega \bullet \mathbf{n}_b < 0. \quad (14.18b)$$

Indeed because we examine the radiative regime in a horizontally extended area the boundary condition (14.13) for the lateral surface ∂V_l is irrelevant. We investigate canopy spectral properties using operator theory (Vladimirov, 1963; Richtmyer, 1978) by introducing the differential, L , and integral, S_λ , operators,

$$\begin{aligned} LI_\lambda &= \Omega \bullet \nabla I_\lambda + G(\mathbf{x}, \Omega) u_L(\mathbf{x}) I_\lambda(\mathbf{x}, \Omega); \\ S_\lambda I_\lambda &= \frac{u_L(\mathbf{x})}{\pi} \int_{\Xi} \Gamma_\lambda(\mathbf{x}, \Omega' \rightarrow \Omega) I_\lambda(\mathbf{x}, \Omega') d\Omega'. \end{aligned} \quad (14.19)$$

The solution I_λ of the boundary value problem (14.3), (14.14) can be represented as the sum of two components, viz., $I_\lambda = Q + \varphi_\lambda$. Here, a *wavelength independent* function Q is the probability density that a photon in the incident radiation will arrive at \mathbf{x} along Ω_0 without suffering a collision. In other words, the function Q describes radiation field generated by *uncollided* photons. It satisfies the equation $LQ = 0$ and the boundary conditions (14.14). Because the uncollided radiation field excludes the scattering event, its solution takes zero values in upward directions. It should be emphasized that the differential operator L does not depend on wavelength and thus Q is *wavelength independent*.

The second term, φ_λ , describes a collided, or diffuse, radiation field; that is, radiation field generated by photons scattered one or more times by phytoelements. It satisfies $L\varphi_\lambda = S_\lambda\varphi_\lambda + S_\lambda Q$ and zero boundary conditions. By letting $K_\lambda = L^{-1}S_\lambda$, the latter can be transformed to

$$\varphi_\lambda = K_\lambda\varphi_\lambda + K_\lambda Q. \quad (14.20)$$

Substituting $\varphi_\lambda = I_\lambda - Q$ into this equation results in an integral equation for I_λ (Vladimirov, 1963; Bell and Glasstone, 1970),

$$I_\lambda = K_\lambda I_\lambda + Q. \quad (14.21)$$

It follows from (14.4.1) that $I_\lambda - K_\lambda I_\lambda$ does not depend on λ , and involves the validity of the following relationship

$$I_\lambda - K_\lambda I_\lambda = I_\nu - K_\nu I_\nu = Q, \quad (14.22)$$

where I_λ and I_ν are solutions of the boundary value problem (14.3), (14.14) at wavelengths λ and ν , respectively. Equation (14.4.1) originally derived by Zhang et al. (2002) expresses the canopy spectral invariant in a general form.

To quantify the spectral invariant, we introduce two coefficients defined as

$$\gamma_0(\lambda) = \frac{\int_V d\mathbf{x} \int_{\Xi} \sigma(\mathbf{x}, \Omega) \varphi_\lambda(\mathbf{x}, \Omega) d\Omega}{\int_V d\mathbf{x} \int_{\Xi} \sigma(\mathbf{x}, \Omega) I_\lambda(\mathbf{x}, \Omega) d\Omega}, \quad (14.23)$$

$$\omega_0(\lambda) = \frac{\int_V d\mathbf{x} \int_{\Xi} \sigma_{s,\lambda}(\mathbf{x}, \Omega) I_{\lambda}(\mathbf{x}, \Omega) d\Omega}{\int_V d\mathbf{x} \int_{\Xi} \sigma(\mathbf{x}, \Omega) I_{\lambda}(\mathbf{x}, \Omega) d\Omega}. \quad (14.24)$$

Here σ and $\sigma_{s,\lambda}$ are the extinction and scattering coefficients; the spatial integration is performed over a sufficiently extended domain V for which the lateral side effects can be neglected. The first coefficient, $\gamma_0(\lambda)$, is the portion of collided radiation in the total radiation field intercepted by a vegetation canopy while the second coefficient, $\omega_0(\lambda)$, is the probability that a photon will be scattered as a result of an interaction within the domain V . We can think of $\omega_0(\lambda)$ as a *mean* single scattering albedo. In general, it can depend on canopy structure, domain V and radiation incident on the vegetation canopy. However, if the leaf albedo (14.6) does not vary with spatial and directional variables, $\omega_0(\lambda)$ coincides with the single scattering albedo $\varpi_{0,\lambda}$.

The ratio

$$p_0 = \gamma_0(\lambda)/\omega_0(\lambda) \quad (14.25)$$

is the probability that a *scattered* photon will hit a leaf in the domain V since $\int_V d\mathbf{x} \int_{\Xi} \sigma(\mathbf{x}, \Omega) \varphi_{\lambda}(\mathbf{x}, \Omega) d\Omega$ is the number of *scattered photons intercepted by leaves* and $\int_V d\mathbf{x} \int_{\Xi} \sigma_{s,\lambda}(\mathbf{x}, \Omega) I_{\lambda}(\mathbf{x}, \Omega) d\Omega$ is the *total number of scattered photons*. This event is determined solely by the structural properties of vegetation which, in turn, are described by the leaf area density and leaf normal orientation distribution functions, each being a wavelength independent variable. This suggests that the probability p_0 should be a wavelength independent variable, too. As it follows from the analysis below, this property is indeed the case!

Let $i(\lambda)$ and $A(\lambda)$ be canopy interception and absorptance defined as

$$i(\lambda) = \frac{\int_V d\mathbf{x} \int_{\Xi} \sigma(\mathbf{x}, \Omega) I_{\lambda}(\mathbf{x}, \Omega) d\Omega}{\int_{\partial V_t} d\mathbf{x}_t \int_{\mathbf{n}_t \bullet \Omega < 0} I_{\lambda}(\mathbf{x}_t, \Omega) |\Omega \bullet \mathbf{n}_t| d\Omega}, \quad (14.26)$$

$$A(\lambda) = \frac{\int_V d\mathbf{x} \int_{\Xi} \sigma_{a,\lambda}(\mathbf{x}, \Omega) I_{\lambda}(\mathbf{x}, \Omega) d\Omega}{\int_{\partial V_t} d\mathbf{x}_t \int_{\mathbf{n}_t \bullet \Omega < 0} I_{\lambda}(\mathbf{x}_t, \Omega) |\Omega \bullet \mathbf{n}_t| d\Omega}.$$

Here σ and $\sigma_{a,\lambda}$ are the extinction and absorption coefficients, respectively. For a vegetation canopy bounded at the bottom by a black surface, $i(\lambda)$ is the average number of photon interactions with the leaves in V before either being absorbed or exiting the domain V . It follows from (14.4.1), (14.4.1) and (??) that

$$\frac{A(\lambda)}{i(\lambda)} = 1 - \omega_0(\lambda). \quad (14.27)$$

This equation has a simple physical interpretation: the capacity of a vegetation canopy for absorption results from the absorption $1 - \omega_0(\lambda)$ of an average leaf multiplied by the average number $i(\lambda)$ of photon interactions with leaves.

Multiplying (14.4.1) by the extinction coefficient σ and integrating over V and all directions Ω and normalizing by the incident radiation flux one obtains

$$i(\lambda) - \gamma_0(\lambda) i(\lambda) = i(\nu) - \gamma_0(\nu) i(\nu) = q. \quad (14.28)$$

Here q is the probability that a photon entering V will hit a leaf. While $1 - q$ is the probability that a photon in the incident radiation will arrive at the canopy bottom without experiencing an interaction with leaves. This probability can be derived from both model calculations and/or field measurements. A question then arises of how $\gamma_0(\lambda)$ can be evaluated?

An eigenvalue of the radiative transfer equation is a number $\tilde{\gamma}(\lambda)$ such that there exists a function $\psi_\lambda(\mathbf{x}, \Omega)$ which satisfies $K_\lambda \psi_\lambda = \tilde{\gamma}(\lambda) \psi_\lambda$. Under some general conditions (Vladimirov, 1963), the set of eigenvalues $\tilde{\gamma}_k, k = 0, 1, 2, \dots$ and eigenvectors $\psi_{\lambda,k}(\mathbf{x}, \Omega), k = 0, 1, 2, \dots$ is a discrete set; the eigenvectors satisfy a condition of orthogonality. The radiative transfer equation has a unique positive eigenvalue which corresponds to a unique positive eigenvector (Vladimirov, 1963). This eigenvalue, say $\tilde{\gamma}_0(\lambda)$, is greater than the absolute magnitudes of the remaining eigenvalues. This means that only one eigenvector, $\psi_{\lambda,0}(\mathbf{x}, \Omega)$, takes on positive values for any \mathbf{x} and Ω . If this positive eigenvector is treated as a source within a vegetation canopy (i.e., uncollided radiation), then $K_\lambda \psi_{\lambda,0}$ describes the collided radiation field. This suggests that the portion, $\gamma_0(\lambda)$, of collided radiation in the total radiation field intercepted by a vegetation canopy can be approximated by the maximum eigenvalue of the radiative transfer equation, i.e., $\gamma_0(\lambda) \approx \tilde{\gamma}_0(\lambda)$. The unique positive eigenvalue $\tilde{\gamma}_0(\lambda)$ can be represented as a product of the mean single scattering albedo $\omega_0(\lambda)$ and a wavelength independent factor $[1 - \exp(-k)]$, i.e., (Knyazikhin and Marshak, 1991)

$$\gamma_0(\lambda) = \omega_0(\lambda) [1 - \exp(-k)]. \quad (14.29)$$

Here k is a coefficient which depends on canopy structure but not on wavelength. Thus, if our hypothesis about the use of the maximum eigenvalue is correct, then the ratio $p_0 = \gamma_0(\lambda)/\omega_0(\lambda)$ does not depend on λ . Substituting $\gamma_0(\lambda) = p_0 \omega_0(\lambda)$ into (14.4.1) and solving for p_0 yields

$$p_0 = \frac{i(\lambda) - i(\nu)}{\omega_0(\lambda) i(\lambda) - \omega_0(\nu) i(\nu)}. \quad (14.30)$$

This equation expresses the canopy spectral invariant for canopy interception; that is the difference between numbers of photons intercepted by the vegetation canopy at two arbitrary wavelengths is proportional to the difference between numbers of scattered photons at the same wavelengths. A similar property is valid for canopy transmittance (Panferov et al., 2001); that is, the quantity

$$p_t = \frac{T(\lambda) - T(\nu)}{\omega_0(\lambda) T(\lambda) - \omega_0(\nu) T(\nu)} \quad (14.31)$$

does not depend on leaf optical properties. Here, the hemispherical canopy transmittance, $T(\lambda)$, for nonisotropic incident radiation is the ratio of the downward radiation flux density at the canopy bottom to the incident radiant,

$$T(\lambda) = \frac{\int_{\partial V_b} d\mathbf{x}_b \int_{\mathbf{n}_b \bullet \Omega > 0} I_\lambda(\mathbf{x}_b, \Omega) |\Omega \bullet \mathbf{n}_t| d\Omega}{\int_{\partial V_t} d\mathbf{x}_t \int_{\mathbf{n}_b \bullet \Omega < 0} I_\lambda(\mathbf{x}_t, \Omega) |\Omega \bullet \mathbf{n}_t| d\Omega}. \quad (14.32)$$

Solving (14.4.1) for $T(\lambda)$ we get

$$T(\lambda) = \frac{1 - p_t \omega_0(\nu)}{1 - p_t \omega_0(\lambda)} T(\nu). \quad (14.33)$$

Similarly, solving (14.4.1) for $i(\lambda)$ and taking into account (14.4.1), we have

$$A(\lambda) = \frac{1 - \omega_0(\lambda)}{1 - \omega_0(\nu)} \frac{1 - p_0 \omega_0(\nu)}{1 - p_0 \omega_0(\lambda)} A(\nu). \quad (14.34)$$

For a vegetation canopy with a non-reflecting surface the determination of canopy transmittance $T(\lambda)$ and absorptance $A(\lambda)$ as a function of wavelength λ follows from these equations in terms of their values at the chosen wavelength ν . The canopy reflectance $R(\lambda)$ (14.3.2) is determined via the energy conservation law as (compare with (8.14) from Chap. 8)

$$T(\lambda) + R(\lambda) + A(\lambda) = 1. \quad (14.35)$$

Panferov et al. (2001) measured spectral hemispherical reflectances and transmittances of individual leaves and the entire canopy to see if (14.4.1) and (14.4.1) hold true. Spectra of $T(\lambda)$ and $R(\lambda)$ in the region from 400 nm to 1100 nm, at 1 nm resolution, were sampled at two sites representative of equatorial rainforests and temperate coniferous forests with a dark ground. A number of leaves from different parts of tree crowns were cut and their spectral transmittances and reflectances (from 400 nm to 1100 nm, at 1 nm resolution) were measured in a laboratory. Mean spectral leaf albedo over collected data was taken as the mean single-scattering albedo $\omega_0(\lambda)$. Given measured $T(\lambda)$, $R(\lambda)$, and $\omega_0(\lambda)$ at 700 different wavelengths, the canopy interception $i(\lambda)$ was evaluated using (14.4.1) and (14.4.1); that is,

$$i(\lambda) = \frac{1 - T(\lambda) - R(\lambda)}{1 - \omega_0(\lambda)}. \quad (14.36)$$

Figure 14.8a shows a cumulative distribution function of p_0 derived from measured values of the right-hand side of (14.4.1) corresponding to all available combinations of λ and ν for which $\lambda > \nu$. One can see that this function is very close to the Heaviside function, with a sharp jump from zero to 1 at $p_0 \approx 0.94$. Its density distribution function behaves as the Dirac delta function. It means that with a very high probability, p_0 is wavelength independent. Solving (14.4.1) for $i(\lambda)$ one obtains

$$i(\lambda) = \frac{1 - p_0 \omega_0(\nu)}{1 - p_0 \omega_0(\lambda)} i(\nu). \quad (14.37)$$

Thus, given canopy interception at an arbitrary chosen wavelength ν , one can evaluate this variable at any other wavelength. Figure 14.8b shows the correlation between canopy interceptions derived from field data directly and evaluated with (14.4.1). One can see that field data follow regularities predicted by (14.4.1) and (14.4.1) and, therefore, do not contradict our hypothesis regarding the maximum eigenvalue of the radiative transfer equation. For details of the mathematical derivation of the canopy spectral invariant for canopy interception and transmittance, the reader is referred to Knyazikhin et al. (1998a) and Panferov et al. (2001).

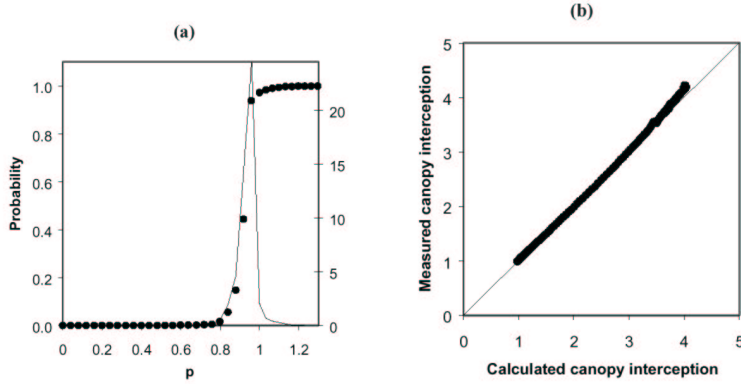


Fig. 14.8. (a) Cumulative distribution function (left axis, dots) and density distribution function (right axis, solid line) of p_0 derived from field data. (b) Correlation between canopy interceptions obtained from Eqs. (14.4.1) and (14.4.1).

14.4.2 Canopy Spectral Behavior in the Case of a Reflective Ground

The canopy spectral invariants discussed in the previous section and the Green's function approach (Sect. 3.10) allow us to fully describe the canopy spectral response to incident solar radiation in terms of a small set of independent variables (Wang et al., 2003). As an example, consider a vegetation canopy layer $0 < z < H$ bounded from below by a Lambertian surface with albedo $\rho_{\lambda,b}$. The plane surfaces $z = 0$ and $z = H$ constitute its upper, ∂V_t , and lower, ∂V_b , boundaries, respectively. Let a parallel beam of intensity I_0 be incident on the upper boundary. The intensity $I_\lambda(\mathbf{x}, \Omega)$ of radiation at the wavelength λ , at a spatial point \mathbf{x} and in direction Ω normalized by I_0 satisfies (14.3) and boundary conditions

$$I_\lambda(\mathbf{x}_t, \Omega) = \delta(\Omega - \Omega_0), \quad \mathbf{x}_t \in \partial V_t, \mu < 0, \quad (14.38a)$$

$$I_\lambda(\mathbf{x}_b, \Omega) = \frac{1}{\pi} \rho_{\lambda,b} \int_{\Xi_-} I_\lambda(\mathbf{x}_b, \Omega') |\mu'| d\Omega', \quad \mathbf{x}_b \in \partial V_b, \mu > 0, \quad (14.38b)$$

where μ and μ' are cosines of zenith angles of Ω and Ω' , respectively and Ξ_- is the downward hemisphere.

The three-dimensional radiation field can be represented as a sum of two components: the radiation calculated for a nonreflecting ("black") surface, $I_{blk,\lambda}(\mathbf{x}, \Omega)$, and the remaining radiation, $I_{rem,\lambda}(\mathbf{x}, \Omega)$; that is,

$$I_\lambda(\mathbf{x}, \Omega) = I_{blk,\lambda}(\mathbf{x}, \Omega) + I_{rem,\lambda}(\mathbf{x}, \Omega). \quad (14.39)$$

The second component, $I_{rem,\lambda}(\mathbf{x}, \Omega)$, accounts for the radiation field due to surface-vegetation multiple interactions and can be expressed as (Sect. 3.10)

$$I_{rem,\lambda}(\mathbf{x}, \Omega) = \rho_{\lambda,b} \int_{\mathbf{x}_b \in \partial V_b} dS(\mathbf{x}_b) F_\lambda(\mathbf{x}_b) J_\lambda(\mathbf{x}, \Omega; \mathbf{x}_b), \quad (14.40)$$

where

$$J_\lambda(\mathbf{x}, \Omega; \mathbf{x}_b) = \frac{1}{\pi} \int_{\Xi_+} d\Omega' G_{S,\lambda}(\mathbf{x}, \Omega; \mathbf{x}_b, \Omega') \quad (14.41)$$

describes the radiation field (in $\text{sr}^{-1}\text{m}^{-2}$) in the canopy layer generated by an isotropic source $\pi^{-1}\delta(\mathbf{x} - \mathbf{x}_b)$ (in $\text{sr}^{-1}\text{m}^{-2}$) located at the point $\mathbf{x}_b \in \partial V_b$, and $G_{S,\lambda}$ is the surface Green function (see Sect. 3.10). The downward radiation flux density at the canopy bottom satisfies the following integral equation (Sect. 3.10)

$$F_\lambda(\mathbf{x}_b) = T_{\text{blk},\lambda}(\mathbf{x}_b) + \rho_{\lambda,b} \int_{\mathbf{x}'_b \in \partial V_b} dS(\mathbf{x}'_b) R_\lambda^*(\mathbf{x}_b, \mathbf{x}'_b) F_\lambda(\mathbf{x}'_b), \quad \mathbf{x}_b \in \partial V_b. \quad (14.42)$$

Here $T_{\text{blk},\lambda}$ is the downward flux density at the canopy bottom calculated for the “black” surface, and $R_\lambda^*(\mathbf{x}_b, \mathbf{x}'_b)$ is downward flux density at $\mathbf{x}_b \in \partial V_b$ generated by the point isotropic source $\pi^{-1}\delta(\mathbf{x} - \mathbf{x}'_b)$ located at $\mathbf{x}'_b \in \partial V_b$.

The use of the Green function allows us to split the radiative transfer problem into two subproblems with purely absorbing boundaries. They are 3D radiation fields generated (a) by the radiation penetrating into the canopy through the upper boundary and (b) by a point isotropic source located at the canopy bottom. The canopy spectral invariant can be applied to each of them. Given solutions of these subproblems, the downward radiation flux density $F_\lambda(x)$ and radiation field $I_{\text{rem},\lambda}(\mathbf{x}, \Omega)$ due to the surface-vegetation multiple interactions can be specified via (14.4.2) and (14.4.2).

In case of horizontally homogeneous vegetation canopy, fluxes F_λ and $F_{\text{blk},\lambda}$ and the probability $R_\lambda^* = \int_{\mathbf{x}'_b \in \partial V_b} dS(\mathbf{x}'_b) R_\lambda^*(\mathbf{x}_b, \mathbf{x}'_b)$ that a photon entering through the lower canopy boundary will be reflected by the vegetation, do not depend on horizontal coordinates and thus a solution to (14.4.2) can be given in an explicit form; that is,

$$F_\lambda = \frac{T_{\text{blk},\lambda}}{1 - \rho_{\lambda,b} R_\lambda^*}. \quad (14.43)$$

Here, $T_{\text{blk},\lambda}$ coincides with the canopy transmittance defined by (14.4.1). It follows from (14.4.2) and (14.4.3) that the solution, $I_\lambda(z, \Omega)$, to the 1D radiative transfer equation can be written as

$$I_\lambda(z, \Omega) = I_{\text{blk},\lambda}(z, \Omega) + \frac{\rho_{\lambda,b}}{1 - \rho_{\lambda,b} R_\lambda^*} T_{\text{blk},\lambda} J_\lambda^*(z, \Omega). \quad (14.44)$$

Here

$$J_\lambda^*(z, \Omega) = \int_{\mathbf{x}_b \in \partial V_b} dS(\mathbf{x}_b) J_\lambda(z, \Omega; \mathbf{x}_b) \quad (14.45)$$

is the radiation field generated by isotropic sources uniformly distributed over surface underneath the vegetation canopy. This decomposition of the radiation field allows the separation of three independent variables responsible for the distribution of solar radiation in vegetation canopies: $\rho_{\lambda,b}$, $I_{\text{blk},\lambda}$ and J_λ^* . The reflectance $\rho_{\lambda,b}$ of

the underlying surface does not depend on the vegetation canopy; $I_{\text{blk},\lambda}$ and J_{λ}^* are surface independent parameters since there is no interaction between the medium and the underlying surface. These variables have intrinsic canopy information.

Let $A_{\text{blk},\lambda}$ and $R_{\text{blk},\lambda}$, defined by (14.4.1) and (14.3.2), be the canopy absorptance and reflectance calculated for the case of the black surface underneath the vegetation canopy. We denote the probabilities that photons from isotropic sources on the canopy bottom will escape the canopy through the upper boundary and be absorbed by the vegetation layer by T_{λ}^* and A_{λ}^* , respectively. These variables can be expressed as

$$T_{\lambda}^* = \int_{\Xi_+} J_{\lambda}^*(H, \Omega) \mu d\Omega, \quad A_{\lambda}^* = \int_0^H dz \int_{\Xi} \sigma_{a,\lambda} J_{\lambda}^*(z, \Omega) d\Omega. \quad (14.46)$$

It follows from here, that the canopy reflectance, R_{λ} , transmittance, T_{λ} , and absorptance, A_{λ} , can be expressed as

$$R_{\lambda} = R_{\text{blk},\lambda} + \frac{\rho_{\lambda,b}}{1 - \rho_{\lambda,b} R_{\lambda}^*} T_{\text{blk},\lambda} T_{\lambda}^*, \quad (14.47a)$$

$$T_{\lambda} = T_{\text{blk},\lambda} + \frac{\rho_{\lambda,b}}{1 - \rho_{\lambda,b} R_{\lambda}^*} T_{\text{blk},\lambda} R_{\lambda}^* = \frac{T_{\text{blk},\lambda}}{1 - \rho_{\lambda,b} R_{\lambda}^*}, \quad (14.47b)$$

$$A_{\lambda} = A_{\text{blk},\lambda} + \frac{\rho_{\lambda,b}}{1 - \rho_{\lambda,b} R_{\lambda}^*} T_{\text{blk},\lambda} A_{\lambda}^*. \quad (14.47c)$$

The canopy spectral invariants can be applied to $A_{\text{blk},\lambda}$, $T_{\text{blk},\lambda}$, T_{λ}^* and A_{λ}^* . The corresponding reflectances $R_{\text{blk},\lambda}$ and R_{λ}^* can be obtained via the energy conservation law; that is,

$$R_{\text{blk},\lambda} + T_{\text{blk},\lambda} + A_{\text{blk},\lambda} = 1, \quad R_{\lambda}^* + T_{\lambda}^* + A_{\lambda}^* = 1. \quad (14.48)$$

Thus, a small set of independent variables generally seems to suffice when attempting to describe the spectral response of a vegetation canopy to incident solar radiation. This set includes the soil reflectance $\rho_{\lambda,b}$, the single scattering albedo, $\omega_0(\lambda)$, canopy transmittance and absorptance at an arbitrary wavelength, and two wavelength independent parameters p_0 and p_t (see (14.4.1) and (14.4.1)) calculated for the black soil problem and for the same canopy illuminated from below by isotropic sources. All of these are measurable parameters. In terms of these variables, solar radiation transmitted, absorbed and reflected by the vegetation canopy at any given wavelength at the solar spectrum can be expressed via Eqs. (14.16) and spectral invariant relations described in Sect. 14.5. Note that a similar statement holds true for non-Lambertian surfaces. For more details on canopy spectral behavior in general case, the reader is referred to (Knyazikhin et al., 1998a,b).

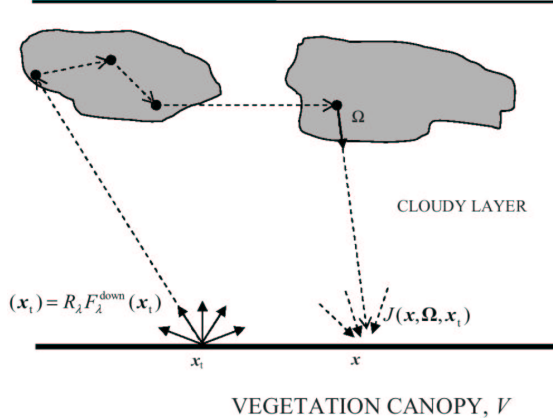


Fig. 14.9. A three-dimensional cloudy layer bounded from below by a horizontally inhomogeneous vegetation canopy, V . Each point on the canopy upper boundary is assumed to reradiate the incident radiation isotropically, i.e., radiant intensity of reflected radiation is independent of direction. The function $J(\mathbf{x}, \Omega, \mathbf{x}_t)$ is the probability that a photon from an isotropic source $1/\pi$ located at \mathbf{x}_t arrives at the point \mathbf{x} along direction Ω as a result of photon-cloud interaction.

14.5 Vegetation Canopy as a Boundary Condition to Atmospheric Radiative Transfer

A decomposition similar to (14.4.2)-(14.4.2) is also valid for the atmosphere (Sect. 3.10) where intensities $I_{\text{blk},\lambda}(\mathbf{x}, \Omega)$ and $I_{\text{rem},\lambda}(\mathbf{x}, \Omega)$ are determined by the atmospheric radiative transfer equation (@ @. @@) in which the canopy bidirectional reflectance factor (BRF, Sect. 14.3.2) appears in the lower boundary condition. The BRF can be parameterized in terms of variables introduced earlier in this chapter. As a result, we have a set of surface and atmosphere variables required to quantitatively describe canopy-cloud interaction. As an example, consider a 3D cloudy layer bounded from below by a horizontally inhomogeneous vegetation canopy, V (Fig. 14.9). We idealize the vegetation canopy as a horizontally inhomogeneous Lambertian surface, i.e., the canopy BRF at a given spatial point \mathbf{x}_t on the canopy top is independent of directions of incident and reflected radiation. For ease of the analysis, we assume that photons can interact only with cloud drops. Keeping this in mind and combining (14.4.2) - (14.4.2), results in

$$I_\lambda(\mathbf{x}, \Omega) = I_{\text{blk},\lambda}(\mathbf{x}, \Omega) + \int_{\mathbf{x}_t \in \partial V_t} F_\lambda^{\text{up}}(\mathbf{x}_t) J_\lambda(\mathbf{x}, \Omega, \mathbf{x}_t) dS(\mathbf{x}_t) \quad (14.49)$$

for any point \mathbf{x} in the cloudy layer or on its lower boundary which is ∂V_t (Fig. 14.9). Here $F_\lambda^{\text{up}}(\mathbf{x}_t)$ is the upward flux density at \mathbf{x}_t , $I_{\text{blk},\lambda}$ is the radiation field in the cloudy layer calculated for a “black” canopy. The term J_λ is the probability that

a photon from an isotropic source $1/\pi$ located at \mathbf{x}_t arrives at the point \mathbf{x} along direction Ω as a result of photon-cloud interaction. Under the above assumptions, J_λ is a surface independent variable. Following (14.4.2) (see also Sect. 3.10),

$$J_\lambda(\mathbf{x}, \Omega, \mathbf{x}_t) = \frac{1}{\pi} \int_{\Xi_-} G_{S,\lambda}(\mathbf{x}, \Omega, \mathbf{x}_t, \Omega') d\Omega' \quad (14.50)$$

where the Green's function $G_{S,\lambda}$ describes the cloud radiative response to the point monodirectional source $\delta(\mathbf{x} - \mathbf{x}_t)\delta(\Omega - \Omega')$ located at the top of the canopy. If the canopy is idealized as a horizontally homogeneous surface, then $F_\lambda^{\text{up}}(\mathbf{x}_t) = R_\lambda F_\lambda^{\text{down}}(\mathbf{x}_t)$ where the canopy reflectance (canopy albedo) R_λ is defined by (14.16).

In contrast to a vegetation canopy, variations in cloud optical properties (single scattering albedo, extinction coefficient and asymmetry factor) in the spectral region between 500 nm and 900 nm are small and, as a first approximation, can be assumed to be wavelength independent. It follows from this assumption that J_λ is also wavelength independent and $I_{\text{blk},\lambda_1} = I_{\text{blk},\lambda_2}$ for any wavelength in this spectral region. Thus,

$$I_{\lambda_1}(\mathbf{x}, \Omega) - I_{\lambda_2}(\mathbf{x}, \Omega) = \int_{\mathbf{x}_t \in \partial V_t} [R_{\lambda_1} F_{\lambda_1}^{\text{down}}(\mathbf{x}_t) - R_{\lambda_2} F_{\lambda_2}^{\text{down}}(\mathbf{x}_t)] J(\mathbf{x}, \Omega, \mathbf{x}_t) dS(\mathbf{x}_t). \quad (14.51)$$

Below we will limit ourselves by considering only points \mathbf{x} located at the top of the canopy, i.e., both \mathbf{x} and \mathbf{x}_t belong to ∂V_t . We first define a bottom-of-atmosphere reflectance (BOAR), $s_\lambda(\mathbf{x}, \Omega)$, for isotropic incident radiation as

$$s_\lambda(\mathbf{x}, \Omega) = \frac{\int_{\mathbf{x}_t \in \partial V_t} F_\lambda^{\text{up}}(\mathbf{x}_t) J(\mathbf{x}, \Omega, \mathbf{x}_t) dS(\mathbf{x}_t)}{F_\lambda^{\text{up}}(\mathbf{x})}. \quad (14.52a)$$

This variable describes cloud-surface interaction as if the cloudy atmosphere be illuminated from below by horizontally heterogeneous isotropic sources of intensity $F_\lambda^{\text{up}}(\mathbf{x})$. For a horizontally homogeneous cloud layer, the upward radiation flux density F_λ^{up} does not depend on position and thus the BOAR coincides with the probability that isotropically illuminated clouds reflect the radiation into direction Ω .

For horizontally inhomogeneous clouds, the downward radiation flux and thus the upward flux density F_λ^{up} can vary significantly. However, it does not necessarily involve large variation in $s_\lambda(\mathbf{x}, \Omega)$. A theoretical explanation of this result can be found in the linear operator analysis (Krein, 1967) and, specifically, in its applications to radiative transfer theory (Knyazikhin, 1991; Kaufmann et al., 2000; Zhang et al., 2002; Lyapustin and Knyazikhin, 2002). One of the theorems of the operator theory states that, for a continuous positive linear operator B , minimum, m_n , and maximum, M_n , values of the function $\eta_n = \sqrt[n]{B^n u}$ converge to the maximum eigenvalue, $\rho(B)$, of the operator B from below and above for any arbitrarily chosen positive function u , i.e., $m_n \leq \rho(B) \leq M_n$ and $M_n - m_n$ tends to zero as n tends to infinity. For the problem of atmospheric radiative transfer over common

land-surface types, including vegetation, soil sand, and snow, the proximity of m_n to M_n to a high accuracy holds at $n \geq 2$ (Lyapustin and Knyazikhin, 2002).

For a given direction Ω , the numerator in (14.17) can be treated as a positive integral operator J with a wavelength independent kernel $J(\mathbf{x}, \Omega, \mathbf{x}_t)$. Its maximum eigenvalue, $\rho(J, \Omega)$, therefore, is also wavelength independent. We approximate the BOAR by the maximum eigenvalue, i.e., $s_\lambda(\mathbf{x}_t, \Omega) \approx \rho(J, \Omega)$.

For a horizontally homogeneous vegetation canopy, (14.5) can therefore be rewritten as

$$\frac{I_{\lambda_1}(\mathbf{x}, \Omega) - I_{\lambda_2}(\mathbf{x}, \Omega)}{R_{\lambda_1}F_{\lambda_1}^{\text{down}}(\mathbf{x}) - R_{\lambda_2}F_{\lambda_2}^{\text{down}}(\mathbf{x})} \approx \rho(J, \Omega). \quad (14.52b)$$

Thus, a simple algebraic combination of radiance, downward flux density, and canopy albedo eliminate their dependencies on wavelength through the specification of a cloud-structure wavelength independent variable. The right-hand side of (14.17) is related to a wavelength independent cloud optical depth above \mathbf{x} . Indeed, it follows from the above mentioned theorem that $\rho(J, \Omega)$ can be estimated from below and above by the minimum and maximum values of the function $\eta_1 = Ju|_{u \equiv 1}$ calculated for $u \equiv 1$. We take this variable as the first approximation to $\rho(J, \Omega)$, i.e.,

$$\rho(J, \Omega) \approx \eta_1 = \int_{\mathbf{x}_t \in \partial V_t} J(\mathbf{x}, \Omega, \mathbf{x}_t) d\mathbf{x}_t. \quad (14.52c)$$

For a plane-parallel geometry, \mathbf{x} -independent $\rho(J, \Omega)$ is nothing else but cloud reflection in the direction Ω from isotropic illumination which is a monotonic function of cloud optical depth.

Assuming that surface measurements of downward radiance and flux densities are available at two wavelengths with the strongest surface contrast (say, red, $\lambda_1 = 0.66 \mu\text{m}$ and NIR, $\lambda_2 = 0.66 \mu\text{m}$), Barker and Marshak (2001); Barker et al. (2002) following Marshak et al. (2000) used the ratio (14.17) to retrieve ρ and thus cloud optical depth above \mathbf{x} for horizontally inhomogeneous even broken clouds. The relationship between ρ and cloud optical depth was approximated using 1D radiative transfer. A modified function J that depends only on a horizontal distance between points where a photon enters and exits a cloud is related to a cloud radiative transfer Green function. Based on diffusion approximation for slab geometry, Chap. 8 shows an analytically derived relationship between cloud optical and geometrical thicknesses from one side, and the horizontal distance of photon travel, from the other.

14.6 Summary

Solar radiation scattered from a vegetation canopy results from interaction of photons traversing through the foliage medium, bounded at the bottom by a radiatively participating surface. To estimate the canopy radiation regime, four important features must be carefully formulated. They are (1) the architecture of individual plants and the entire canopy; (2) optical properties of vegetation elements (leaves,

stems), (3) reflective properties of the ground underneath the canopy and (4) atmospheric conditions. Photon transport theory aims at deriving the solar radiation regime within the vegetation canopy using the above mentioned attributes as input. The first two attributes are accounted in the extinction and differential scattering coefficients which appear in the radiative transfer equation. Their specification requires models for the leaf area density function, the probability density of leaf normal orientation, and the leaf scattering phase function (Sect. 14.2). Reflective properties of the ground and atmospheric conditions determine the boundary conditions for the radiative transfer equation required to describe incoming radiation and radiation reflected by the ground. A solution of the boundary value problem describes the radiative regime in a vegetation canopy and, as a consequence, its reflective properties (Sect. 14.3). The latter, for example, is required to specify boundary conditions for the transfer of radiation in a cloudy atmosphere adjoining a vegetation canopy (Sect. 14.5).

In contrast to radiative transfer in clouds, the extinction coefficient in vegetation canopies does not depend on wavelength. This feature results in canopy spectral invariants; that is, some simple algebraic combinations of the single scattering albedo and canopy spectral transmittances and reflectances eliminate their dependencies on wavelength through the specification of canopy structure dependent variables. These variables are related to the maximum positive eigenvalues of linear operators describing the canopy transmittance and radiation field in the vegetation canopy. The eigenvalues have a simple physical interpretation. They represent the collided radiation portions of the total transmitted and intercepted radiation. In terms of the maximum eigenvalues, the partitioning of the incident solar radiation into canopy transmission and absorption can be described by expressions which relate canopy transmittance and interception at an arbitrarily chosen wavelength to transmittances and interceptions at any other wavelength in the solar spectrum. Furthermore, the canopy spectral invariant allows us to separate a small set of independent variables that fully describe the law of energy conservation in vegetation canopies at any given wavelength in the solar spectrum (Sect 14.4). This feature of the solution of the canopy radiative transfer equation provides an accurate parameterization of the boundary value problem for the radiative transfer in a cloudy atmosphere adjoining the vegetation canopy (Sect.14.5). Finally we showed that interactions between vegetation and horizontally inhomogeneous clouds can be exploited to retrieve cloud optical depth from ground-based radiance measurements.

References

- Antyufeev, V. and A. Bondarenko (1996). X-ray tomography in scattering media. *SIAM J. Appl. Math.*, **56**, 573–587.
- Barker, H. and A. Marshak (2001). Inferring Optical Depth of Broken Clouds Above Green Vegetation Using Surface Solar Radiometric Measurements. *J. Atmos. Sci.*, **58**, 2989–3006.

- Barker, H., A. Marshak, W. Szyrmer, A. Trishchenko, J.-P. Blanchet, and Z. Li (2002). Inference of cloud optical properties from aircraft-based solar radiometric measurements. *J. Atmos. Sci.*, **59**, 2093–2111.
- Bell, G. and S. Glasstone (1970). *Nuclear Reactor Theory*. Van Nostrand Reinhold, New York (NY).
- Bréon, F.-M., F. Maignan, M. Leroy, and I. Grant (2001). A statistical analysis of Hot Spot directional signatures measured from space. *8th Internationsl Symposium Physical Measirements and Signatures in Remote Sensing, Aussois, France*, pages 343–353.
- Bunnik, N. (1978). *The multispectral reflectance of shortwave radiation by agricultural crops in relation with their morphological and optical properties*. Pudoc Publications, Wageningen, The Netherlands.
- Choulli, M. and P. Stefanov (1996). Reconstruction of the coefficient of the stationary transport equation from boundary measurements. *Inverse Problems*, **12**, L19–L23.
- Deschamps, P., F. Bréon, M. Leroy, A. Podaire, A. Bricaud, J. Buriez, and G. Sèze (1994). The POLDER mission: Instrument characteristics and scientific objectives. *IEEE Trans. Geosci. Remote Sens.*, **32**, 598–615.
- DeWit, C. (1965). Photosynthesis of leaf canopies. Technical Report Agric. Res. Report 663, Pudoc Publ., Wageningen, The Netherlands.
- Diner, D., G. Asner, R. Davies, Y. Knyazikhin, J. Muller, A. Nolin, B. Pinty, C. B. Schaaf, and J. Stroeve (1999). New directions in Earth observing: Scientific application of multi-angle remote sensing. *Bull. Amer. Meteorol. Soc.*, **80**, 2209–2228.
- Germogenova, T. (1986). *The Local Properties of the Solution of the Transport Equation (in Russian)*. Nauka, Moscow, Russia.
- Gerstl, S. and C. Simmer (1986). Radiation physics and modeling for off-nadir satellite-sensing of non-Lambertian surfaces. *Remote Sens. Environ.*, **20**, 1–29.
- Goel, N. and D. Strelbel (1984). Simple Beta distribution representation of leaf orientation in vegetation canopies. *Agron. J.*, **76**, 800–802.
- Intergovernmental Panel on Climate Change (IPCC) (1995), Houghton, J., L. M. Filho, B. Callander, N. Harris, A. Kattenberg, and K. Maskell, editors, *Climate Change: Report of the Intergovernmental Panel on Climate Change (IPCC)*. Cambridge University Press, New York, (NY).
- Kaufmann, R., L. Zhou, Y. Knyazikhin, N. Shabanov, R. Myneni, and C. Tucker (2000). Effect of orbital drift and sensor changes on the time series of AVHRR vegetation index data. *IEEE Trans. Geosci. Remote Sens.*, **38**, 2584–2597.
- Knyazikhin, Y. (1991). On the Solvability of Plane-Parallel Problems in the Theory of Radiation Transport. *USSR Computer Maths. and Math. Phys., English version*, **30**, 145–154.
- Knyazikhin, Y. and A. Marshak (1991), Myneni, R. and J. Ross, editors, *Fundamental equations of radiative transfer in leaf canopies and iterative methods for their solution*, pages 9–43. Springer-Verlag, New York (NY).
- Knyazikhin, Y., A. Marshak, D. Schulze, R. Myneni, and G. Gravenhorst (1994). Optimisation of Solar Radiation Input in Forest Canopy as a Tool for Planting Patterns of Trees. *Transport Theory and Statist. Phys.*, **23**, 671–700.

- Knyazikhin, Y., J. Kranigk, G. Miessen, O. Panfyorov, N. Vygodskaya, and G. Gravenhorst (1996). Modelling Three-Dimensional Distribution of Photosynthetically Active Radiation in Sloping Coniferous Stands. *Biomass and Bioenergy*, **11**, 189–200.
- Knyazikhin, Y., G. Miessen, O. Panfyorov, and G. Gravenhorst (1997). Small-Scale study of three-dimensional distribution of photosynthetically active radiation in a forest. *Agric. For. Meteorol.*, **88**, 215–239.
- Knyazikhin, Y., J. Martonchik, D. Diner, R. Myneni, M. Verstraete, B. Pinty, and N. Gobron (1998a). Estimation of vegetation canopy leaf area index and fraction of absorbed photosynthetically active radiation from atmosphere corrected MISR data. *J. Geophys. Res.*, **103**, 32,239–32,256.
- Knyazikhin, Y., J. Martonchik, R. Myneni, D. Diner, and S. Running (1998b). Synergistic algorithm for estimating vegetation canopy leaf area index and fraction of absorbed photosynthetically active radiation from MODIS and MISR data. *J. Geophys. Res.*, **103**, 32,257–32,276.
- Kranigk, J. (1996). *Ein Model für den Strahlungstransport in Fichtenbeständen*. Cuvillier, Göttingen, Germany.
- Kranigk, J. and G. Gravenhorst (1993). Ein dreidimensionales Modell für Fichtenkronen. *Allg. Forst Jagdztg.*, **164**, 146–149.
- Kranigk, J., F. Gruber, J. Heimann, and A. Thorwest (1994). Ein Model für die Kronenraumstruktur und die räumliche Verteilung der Nadeloberfläche in einem Fichtenbestand. *Allg. Forst Jagdztg.*, **165**, 193–197.
- Krein, S., editor (1967). *Functional Analysis*. Foreign Technol. Div., Wright-Patterson Air Force Base, Ohio.
- Kuusk, A. (1985). The hot spot effect of a uniform vegetative cover. *Sov. J. Remote Sens.*, **3**, 645–658.
- Lyapustin, A. and Y. Knyazikhin (2002). Green's function method for the radiative transfer problem. 2. Spatially heterogeneous anisotropic surface. *Applied Optics*, **41**, 5600–5606.
- Marshak, A. (1989). Effect of the hot spot on the transport equation in plant canopies. *J. Quant. Spectrosc. Radiat. Transfer*, **42**, 615–630.
- Marshak, A., Y. Knyazikhin, A. Davis, W. Wiscombe, and P. Pilewskie (2000). Cloud - Vegetation Interaction: Use of Normalized Difference Cloud Index for Estimation of Cloud Optical Thickness. *Geophys. Res. Lett.*, **27**, 1695–1698.
- Martonchik, J., C. Bruegge, and A. Strahler (2000). A review of reflectance nomenclature used in remote sensing. *Remote Sensing Reviews*, **19**, 9–20.
- Myneni, R. (1991). Modeling radiative transfer and photosynthesis in three-dimensional vegetation canopies. *Agric. For. Meteorol.*, **55**, 323–344.
- Myneni, R., G. Asrar, and S. Gerstl (1990). Radiative transfer in three dimensional leaf canopies. *Transp. Theor. Stat. Phys.*, **19**, 205–250.
- Myneni, R., S. Hoffman, Y. Knyazikhin, J. Privette, J. Glassy, Y. Tian, Y. Wang, X. Song, Y. Zhang, G. Smith, A. Lotsch, M. Friedl, J. Morisette, P. Votava, R. Nemani, and S. Running (2002). Global products of vegetation leaf area and fraction absorbed par from year one of MODIS data. *Remote Sens. Environ.*, **83**, 214–231.

- Panferov, O., Y. Knyazikhin, R. Myneni, J. Szarzynski, S. Engwald, K. Schnitzler, and G. Gravenhorst (2001). The role of canopy structure in the spectral variation of transmission and absorption of solar radiation in vegetation canopies. *IEEE Trans. Geosci. Remote Sens.*, **39**, 241–253.
- Pinty, B. and M. Verstraete (1997). Modeling the scattering of light by vegetation in optical remote sensing. *J. Atmos. Sci.*, **55**, 137–150.
- Richtmyer, R., editor (1978). *Principles of Advanced Mathematical Physics*, volume 1. Springer-Verlag, New York (NY).
- Ross, J., editor (1981). *The Radiation Regime and Architecture of Plant Stands*. Dr. W. Junk, Norwell (MA).
- Shabanov, N., Y. Wang, W. Buerman, J. Dong, S. Hoffman, G. Smith, Y. Tian, Y. Knyazikhin, and R. Myneni (2003). Effect of Foliage Spatial Heterogeneity on the MODIS LAI and FPAR Algorithm over Broadleaf Forests. *Remote Sens. Environ.*, **85**, 410–423.
- Steffen, W., I. Noble, J. Canadell, M. Apps, E. Schulze, P. Jarvis, D. Baldocchi, P. Ciais, W. Cramer, J. Ehleringer, G. Farquhar, C. Field, A. Ghazi, R. Gifford, M. Heimann, R. Houghton, P. Kabat, C. Körner, E. Lambin, S. Linder, H. Mooney, D. Murdiyarso, W. Post, I. Prentice, M. Raupach, D. Schimel, A. Shvidenko, and R. Valentini (1998). The terrestrial carbon cycle: Implications for the Kyoto Protocol. *Science*, **280**, 1393–1397.
- van de Hulst, H. (1980). *Multiple Light Scattering: Tables, Formulae and Applications*, volume I. Academic Press, San Diego, CA.
- Vanderbilt, V., L. Grant, and S. Ustin (1991), Myneni, R. and J. Ross, editors, *Polarization of light by vegetation*, pages 191–228. Springer Verlag, New York, USA.
- Verstraete, M. (1987). Radiation transfer in plant canopies: transmission of direct solar radiation and the role of leaf orientation. *J. Geophys. Res.*, **92**, 10,985–10,995.
- Verstrate, M., B. Pinty, and R. Dickinson (1990). A physical model of the bidirectional reflectance of vegetation canopies. 1. Theory. *J. Geophys. Res.*, **95**, 11,755–11,765.
- Vladimirov, V. (1963). Mathematical problems in the one-velocity theory of particle transport. Technical Report AECL-1661, At. Energy of Can. Ltd.
- Walter-Shea, E. and J. Norman (1991), Myneni, R. and J. Ross, editors, *Leaf optical properties*, pages 229–251. Springer-Verlag, New York, USA.
- Wang, Y., W. Buermann, P. Stenberg, P. Voipio, H. Smolander, T. Häme, Y. Tian, J. Hu, Y. Knyazikhin, and R. Myneni (2003). A New Parameterization of Canopy Spectral Response to Incident Solar Radiation: Case Study with Hyperspectral Data from Pine Dominant Forest. *Remote Sens. Environ.*, **85**, 304–315.
- Zhang, Y., N. Shabanov, K. Y, and R. Myneni (2002). Assessing the information content of multiangle satellite data for mapping biomes. II. Theory. *Remote Sens. Environ.*, **80**, 435–446.

Suggested Reading

Ross, J. (1981). *The Radiation Regime and Architecture of Plant Stands*. Dr. W. Junk, Norwell, Mass., USA, 391pp.

This is a classical monograph in which Juhan Ross originally formulated radiative transfer in vegetation canopies as a problem in mathematical physics as well as parameterized the architecture of the vegetation canopy and optical properties of vegetation elements in terms of the leaf area density function, the probability density of leaf normal orientation, and the leaf scattering phase function. He also provided a solution of the radiative transfer for several special cases.

Myneni, R.B. and Ross, J. (Eds.) (1991). *Photon-Vegetation Interactions: Applications in Plant Physiology and Optical Remote Sensing*. Springer-Verlag, New York, USA, 565pp.

This monograph summarizes progress in the radiative transfer theory for plant canopies since the publication of Ross' book. This edited monograph consists of 17 chapters that present new approaches to the boundary value problem for radiative transfer equation in vegetation canopies, new numerical and analytical methods of its solution. A special emphasis is given to the application of the theory in the plant ecology and optical remote sensing.

Kuusk, A. (1985). The hot spot effect of a uniform vegetative cover. *Sov. J. Remote Sens.*, **3**, 645-658.

Simmer, C. and S.A. Gerstl (1985). Remote sensing of angular characteristics of canopy reflectances. *IEEE Trans. Geosci. Remote Sens.*, **GE-23**, 648-658.

Marshak, A. (1989). Effect of the hot spot on the transport equation in plant canopies. *J. Quant. Spectrosc. Radiat. Transfer*, **42**, 615-630.

Verstraete M.M., B. Pinty, and R.E. Dickenson (1990). A physical model of the bidirectional reflectance of vegetation canopies. 1. Theory. *J. Geophys. Res.*, **95**, 11,765-11,775.

Myneni, R.B. and G. Asrar (1991). Photon interaction cross sections for aggregations of finite dimensional leaves. *Remote Sens. Environ.*, **37**, 219-224.

Pinty, B. and M.M. Verstraete (1997). Modeling the scattering of light by vegetation in optical remote sensing. *J. Atmos. Sci.*, **55**, 137-150.

The hot spot effect (Fig. 14.1) is a result of cross-shading between finite dimensional leaves in the canopy leading to a peak in reflectance in the retro-illumination direction. The radiative transfer equation in its original formulation (Ross, 1981) fails to predict or duplicate this effect. These papers present models of the canopy bidirectional reflectance factor which account for the hot spot effect.

Knyazikhin, Y., J.V. Martonchik, D.J.Diner, R.B. Myneni, M.M. Verstraete, B.Pinty, and N. Gobron (1998). Estimation of vegetation canopy leaf area index and fraction of absorbed photosynthetically active radiation from atmosphere corrected MISR data. *J. Geophys. Res.*, **103**, 32,239-32,256.

Knyazikhin, Y., J.V. Martonchik, R.B. Myneni, D.J. Diner, and S.W. Running (1998). Synergistic algorithm for estimating vegetation canopy leaf area index and fraction of absorbed photosynthetically active radiation from MODIS and MISR data. *J. Geophys. Res.*, **103**, 32,257-32,276.

These papers describe the operational algorithm of global LAI (leaf area index) and FPAR (the fraction of photosynthetically active radiation, 400 nm-700 nm) absorbed by vegetation for the MODIS (Moderate Resolution Imaging Spectroradiometer) and MISR (Multiangle Imaging Spectroradiometer) instruments of the Earth Observing System Terra mission. Theory of radiative transfer in vegetation canopies presented in this chapter underlies this algorithm. It is also shown in the second paper that a rather wide family of canopy radiation models designed to account for the hot spot effect conflict with the law of energy conservation. This law was taken as a basic tool to constrain retrievals in the MODIS/MISR LAI/FPAR retrieval techniques. A theoretical derivation of the canopy spectral invariants was originally presented in these papers.

Zhang, Y., Y. Tian, R.B. Myneni, Y. Knyazikhin, and C.E. Woodcock (2002). Assessing the information content of multiangle satellite data for mapping biomes. I. Statistical Analysis. *Remote Sens. Environ.*, **80**, 418-434.

Zhang, Y., N. Shabanov, Y. Knyazikhin, and R.B. Myneni (2002). Assessing the information content of multiangle satellite data for mapping biomes. II. Theory. *Remote Sens. Environ.*, **80**, 435-446.

Knyazikhin, Y., A. Marshak, W.J. Wiscombe, J. Martonchik, and R.B. Myneni (2002). A missing solution to the transport equation and its effect on estimation of cloud absorptive properties. *J. Atmos. Sci.*, **59**, 3572-3585.

It is shown in the first two papers that if the solution to the radiative transfer equation is treated as a Schwartz distribution, then an additional term must be added to the solution of the radiative transfer equation. This term describes the hot spot effect. A similar result takes place in cloud radiative transfer; this is documented in the third paper.

Panferov, O., Y. Knyazikhin, R.B. Myneni, J. Szarzynski, S. Engwald, K.G. Schnitzler, and G. Gravenhorst (2001). The role of canopy structure in the spectral variation of transmission and absorption of solar radiation in vegetation canopies. *IEEE Trans. Geosci. Remote Sens.*, **39**, 241-253.

Wang, Y., W. Buermann, P. Stenberg, P. Voipio, H. Smolander, T. Häme, Y. Tian, J. Hu, Y. Knyazikhin, and R. B. Myneni (2003). A new parameterization of canopy spectral response to incident solar radiation: Case study with hyperspectral data from pine dominant forest. *Remote Sens. Environ.*, **85**, 304-315.

Shabanov, N.V., Y. Wang, W. Buerman, J. Dong, S. Hoffman, G.R. Smith, Y. Tian, Y. Knyazikhin, and R.B. Myneni (2003). Effect of foliage heterogeneity on the MODIS LAI and FPAR over broadleaf forests. *Remote Sens. Environ.*, **85**, 410-423.

An experimental derivation of the canopy spectral invariants as well as their use in parameterization of canopy spectral response to incident solar radiation is discussed in these papers.

- Marshak, A., Yu. Knyazikhin, A. Davis, W. Wiscombe, and P. Pilewskie (2000). Cloud Vegetation interaction: Use of normalized difference cloud index for estimation of cloud optical thickness. *Geoph. Res. Lett.*, **27**, 1695-1698.
- Knyazikhin, Yu., and A. Marshak (2000). Mathematical aspects of BRDF modeling: Adjoint problem and Green's function. *Remote Sens. Review*, **18**, 263-280.
- Barker, H., and A. Marshak (2001). Inferring optical depth of broken clouds above green vegetation using surface solar radiometric measurements. *J. Atmos. Sci.*, **58**, 2989-3006.

These papers discuss cloud-vegetation interactions and derive a Green's function as a cloud radiative response to the illumination by a point monodirectional source located on the vegetated surface. They also propose a method for inferring cloud optical depth for inhomogeneous clouds using surface-based radiometric observations at two wavelengths with the strongest surface contrast and similar cloud optical properties. A special emphasis is given to the case of broken clouds.